

# Results of a round robin measurement on a new CD mask standard

Th. Schätz<sup>1</sup>, F. Gans<sup>2</sup>, R. Liebe<sup>2</sup>, J. Richter<sup>2</sup>, B. Hauße<sup>3</sup>, F. Hillmann<sup>4</sup>, S. Döbereiner<sup>4</sup>, H.-J. Brück<sup>4</sup>, G. Scheuring<sup>4</sup>, B. Brendel<sup>5</sup>, L. Bettin<sup>5</sup>, K.-D. Röth<sup>6</sup>, W. Steinberg<sup>6</sup>, G. Schlüter<sup>6</sup>, P. Speckbacher<sup>7</sup>, W. Sedlmeier<sup>7</sup>, T. Scherübl<sup>8</sup>, W. Häßler-Grohne<sup>9</sup>, C.G. Frase<sup>9</sup>, S. Czerkas<sup>9</sup>, K. Dirscherl<sup>9</sup>, B. Bodermann<sup>9</sup>, W. Mirandé<sup>9</sup>, H. Bosse<sup>9</sup>

<sup>1</sup>Infinitec Technologies AG, D-81541, München, <sup>2</sup>AMTC, D-01109 Dresden, <sup>3</sup>Photronics MZD GmbH & Co. KG, D-01109 Dresden, <sup>4</sup>MueTec GmbH, D-80993 München, <sup>5</sup>Leica Microsystems Lithography GmbH, D-07745 Jena, <sup>6</sup>Leica Microsystems Wetzlar GmbH, D-35578 Wetzlar, <sup>7</sup>Dr. Johannes Heidenhain GmbH, D-83301 Traunreut, <sup>8</sup>Carl Zeiss Jena GmbH, D-07745 Jena, <sup>9</sup>Physikalisch-Technische Bundesanstalt (PTB), D-38116 Braunschweig, all from Germany  
(e-mail: Harald.Bosse@ptb.de)

## ABSTRACT

We report on the results of a recent round robin comparison on new linewidth or CD photomask standards in which several partners from different companies and institutes in Germany were involved. The round robin activity is at the end of a joint project targeting at the development of a new CD mask standard and it was intended to show the performance of the CD mask standard and to test its application in cross-calibration processes. Different type of CD metrology instrumentation was used, namely optical transmission microscopy including water immersion CD microscopes with NA of 1.2 and scanning electron microscopy, supported by additional scanning probe microscopy (SPM/AFM) characterizations. A set of differently processed CD mask standards with smallest line and space structures down to 0.1  $\mu\text{m}$  and based on different mask blanks was produced with identical layout. At the PTB this set of CD standards was calibrated by UV transmission microscopy and by CD-SEM as well. For the round robin an unknown CD mask of the same design as the standards was used and the participants were asked to provide measurement data with their CD metrology tools, referred to their respective PTB calibration standards. It will be shown, that the agreement of measurement data between different CD metrology tools can be significantly improved if proper definitions of the measurand and a metrologically sound approach to signal modelling and interpretation of CD measurement values is applied. The outcome of this comparison provides a valuable source of information for cross calibration issues which are discussed in mask industry today and, moreover, it proves the performance of the newly developed CD mask standard, which now is available to other interested parties, too.

Keywords: SEM, UV transmission microscopy, CD metrology, photomask standard, signal modelling

## 1. INTRODUCTION

This contribution reports on the final results of a project about the definition, development, calibration and application of a new CD photomask standard initiated by the PTB together with several industrial partners from Germany. Photomasks are and will also be in the (near) future the essential elements in the lithographic manufacturing process of electronic components. Chrome on glass (COG) or binary masks consist of a quadratic substrate of quartz glass with the physical dimensions 152 mm x 152 mm x 6.35 mm and an antireflective chromium layer of usually less than 100 nm thickness. The chromium layer is typically structured by high resolution electron beam lithography and represents the structures which have to be transferred to the wafer. Although typically the dimensions of the structures on the masks are de-magnified by the lithographic projection lens system by a factor of 1:4, masks currently produced contain structures as small as the sub-100nm functional structures on the wafer. These so-called OPC structures (optical proximity correction) are used on the masks to enhance the quality of lithographic reproduction. In addition to OPC techniques, phase shifting masks (PSM) nowadays are widely used to achieve the required resolution and process capability in lithographic production.

In order to reliably produce masks with smallest structures down to 100 nm or even smaller, corresponding CD calibration standards, verified calibration methods and a prove of applicability of these methods and standards in industrial quality control processes are necessary. The project described here for development and calibration of new CD standards tried to address these requirements. In particular, a comparison of different CD measurement methods like UV transmission microscopy, low voltage SEM and AFM requires a detailed analysis of the physical interaction processes leading to the formation of characteristic contrasts and signal profiles that are used for CD evaluation. In prior measurements [1], optical measurement results were used as a reference for the offset correction of all other measurement methods. Now, for every measurement method independent and traceable measurement results with measurement uncertainty estimation were specified. Moreover, new and extended CD measurands like top linewidth are introduced.

## 2. LAYOUT OF MASK STANDARDS

On the 6025 mask, a 3x3 grid of 9 identical dies with 40 mm die size was chosen. For alignment purposes NIKON fiducials were used, and an additional regular pattern of auxiliary alignment crosses was placed near the mask edges, see Fig. 1. During prototype development all 9 dies served for variation of process parameters to obtain information for optimized structure quality. On final masks, only structures within the central die will be calibrated. The other dies can be used to transfer measurement results for everyday calibration purposes or they can be calibrated later if e.g. the central die has been damaged. Within the 40 mm die there are 4 different areas (see Fig. 2): two quarters show the CD test structures in horizontal and in vertical orientation, within the third quarter are different pitch structures and additional 1D-grating structures for scatterometry analysis and the fourth quarter contains a larger transparent field for 100 % transmission reference calibration along with additional line and space structures in non-orthogonal orientation. The pitch structures each consist of 26 lines and spaces (1:1) with the following nominal pitch values: 10  $\mu\text{m}$ , 4  $\mu\text{m}$ , 2  $\mu\text{m}$ , 1  $\mu\text{m}$ , and 0.4  $\mu\text{m}$ . Within each of the two quadrants containing the CD test structures, there are two blocks of structures, one for smallest CDs up to 5  $\mu\text{m}$  and one for larger CDs up to 500  $\mu\text{m}$ . The CD steps are as follows:

55 fine-CD test structure groups: CD from 100 nm to 5 $\mu\text{m}$ with 200 $\mu\text{m}$ pitch	18 coarse-CD test structure groups: CD from 5 $\mu\text{m}$ to 500 $\mu\text{m}$ with 1 mm pitch
<ul style="list-style-type: none"> <li>• 100 ... 500 nm, step 20 nm = 21 groups</li> <li>• 540 ... 900 nm, step 40 nm = 10 groups</li> <li>• 1000 ... 1600 nm, step 100 nm = 7 groups</li> <li>• 1800 ... 5000 nm, step 200 nm = 17 groups</li> </ul>	<ul style="list-style-type: none"> <li>• 6 ... 10 <math>\mu\text{m}</math>, step 1 <math>\mu\text{m}</math> = 5 groups</li> <li>• 20... 50 <math>\mu\text{m}</math>, step 10 <math>\mu\text{m}</math> = 4 groups</li> <li>• 100 ... 500 <math>\mu\text{m}</math>, step 50 <math>\mu\text{m}</math> = 9 groups</li> </ul>

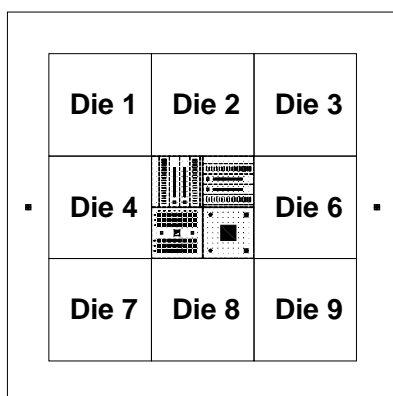


Fig. 1 Overview of mask layout.

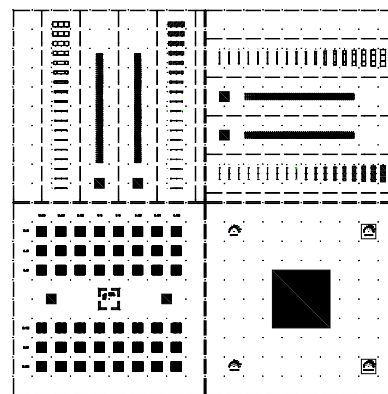
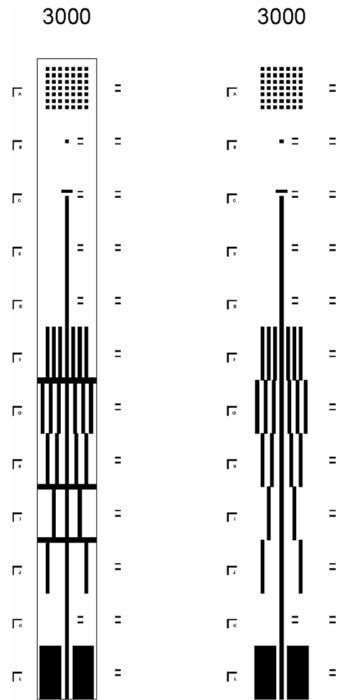


Fig. 2 Die layout of new mask standard.

The basic layout of the smaller CD test structure groups is shown in Fig. 3 exemplarily by means of the nominal 3  $\mu\text{m}$  structure group. It consists of a main line structure in isolated as well as differently dense environments (1:1...1:5) and a square pattern, again isolated as well as grouped. Each of the 12 structure elements uses an area of 50  $\mu\text{m}$  x 50  $\mu\text{m}$ . The structures are identified by label fields (A-L) and alignment L-bars at the left. In addition to this and also for assistance during measurement, the measurement window size of 5  $\mu\text{m}$  height is indicated by two auxiliary lines next to the measurement sections.



**Fig. 3** Layout of CD test structure group; black: quartz, white: chromium (top: clear structures, down: opaque structures).

The opaque line structures are conductively linked to the chromium coverage on the mask to reduce residual charging effects during e-beam measurement. For this, additional Cr lines are arranged perpendicular to realize electrical contact of the opaque measurement line structures with the surrounding chromium film, see Fig. 3. The design of the CD standard is hierarchically structured, which allows to easily remove parts of the design before writing the mask if certain subsets of test structures are not required for the specific application in question.

### 3. CD INSTRUMENTATION AND SIGNAL MODELLING APPROACHES

For the round robin measurements on the COG CD mask standard different type of instrumentation was used by the project partners. DUV/UV optical transmission microscopy and CD-SEM, supported by additional AFM measurements were applied. The PTB provided calibrated CD photomask standards with the design described above, which were used by the round robin participants as CD references for their measurements on the unknown round robin mask. All participants were asked to apply their usual calibration procedures to transfer the results from their CD reference masks to the round robin mask and to finally provide the measurement values.

Two UV (Leica LWM250 UV, MueTec 2010 NT) and two DUV transmission microscopy CD tools (Leica LWM270 DUV, MueTec <M5k>) and two CD-SEM tools (HOLON EMU 220A) were used by the participants. In addition to this, first - however not yet calibrated - measurements by means of a new water immersion DUV tool with NA of 1.2 were performed (LWM 500 WI) [2]. The measurements were supported by characterizations of CD and edge profile and slope by AFM (Park Scientific Autoprobe M5). Furthermore, along with the other instrumentation an AIMS 193 fab tool was used to perform additional measurements on a 193nm attenuated phase shifting mask with identical layout as the COG mask standards.

The instrumentation used at the PTB for the calibration tasks as well as the developed signal modelling approaches to correlate the measured signal with the edge topography of the absorber structures will be described below. The overall objective of the PTB activities in the area of CD photomask metrology is to provide CD or feature width [3] measurement values which are clearly and consistently defined by referring to the topography of the functional structures on the mask and which are traceable to the SI unit of length. However, as demonstrated by inclusion of the AIMS tool in our activities, we also realize that for precise CD control of the printed structures on the wafer a purely dimensional approach for photomask qualification might not be sufficient, especially in the case of PSM.

#### 3.1 UV transmission microscopy at PTB

##### Operation principle

For the optical characterization of the CD photomask standards a special UV transmission microscope calibration system is used [4]. The system is based on a modified commercial microscope (Zeiss Axiotron), equipped with a computer controlled precision sample stage of the double-parallel spring type. The movement of the piezo driven stage is measured both by a high resolution capacitive sensor and an interferometer with a resolution of 0.1 nm and 2 nm, respectively and an uncertainty of 2 nm. The sample is imaged using Koehler illumination ( $NA_C = 0.2$ ) at a wavelength of 365 nm. A slit aperture ( $10 \mu\text{m} \times 1 \text{mm}$ ) placed in the image plane is imaged into the object plane by the microscope objective (magnification 150x,  $NA_O = 0.9$ ). The movement scans the sample over the image of the stationary slit in the microscope light path. The light passing the slit is detected by a photomultiplier and registered together with the signal of the capacitive sensor and the interferometer. The edge position is deduced from the measured signal profile using a threshold criterion based on a suitable physical imaging model.

## Physical modelling

To deduce the edge position from the microscope image a sophisticated imaging model has to be applied, which takes into account the vector characteristics of the electromagnetic field. We use the rigorous coupled wave analysis (RCWA) method [5-7] for image modelling. For this purpose we use the program package MICROSIM developed at the University of Stuttgart, Germany [8]. Simulations based on the RCWA method are used to determine the correct threshold in dependence of the parameters of the imaging system and of the sample.

## CD uncertainty evaluation

The dependence of the correct threshold criterion on the set of the parameters both of the imaging system and the sample will influence the measurement uncertainty. According to [9], all input parameters which significantly influence the final measurement value have to be analysed to set up a complete uncertainty analysis. Therefore we conducted systematic theoretical investigations of the influences of these parameters on the threshold, see details given in [10]. For our UV microscope, a variation of the threshold of 1 % corresponds to a variation of the deduced linewidth of about 4 nm. Our uncertainty analysis results in achievable calibration uncertainties of about 25 nm ( $k = 2$ , 95% confidence interval). This uncertainty was evaluated for a CD, defined as the feature width at 50 % height of the structure, taking into account the actually measured edge slope. The largest uncertainty contributions are due to the instrument itself, the imperfect knowledge of mask material parameters (especially the absorption coefficient of the absorber layer) and the uncertainty of the applied RCWA model itself. This last issue is currently addressed by a running software model comparison for high resolution microscopy on the basis of suitable test suites [11]. Another uncertainty evaluation for CD optical microscopy is given in [12].

It is of special interest to investigate two parameter influences in more detail, which are both due to properties of the COG mask absorption layer itself, namely the thickness of the layer and the edge angle. These parameters also have varied between the different CD reference masks the PTB has calibrated for the participants of the round robin. Figure 4 shows the dependence of the threshold criterion on the thickness of the chromium layer. For typical Cr layer thickness of the mask standards developed within this project of 70–80 nm, we obtain a coefficient of about 0.17 %/nm. The thickness of the chromium layer can be measured using an AFM with an uncertainty of about 2 nm. Thus the uncertainty of layer thickness will result in a linewidth error of about 0.8 nm.

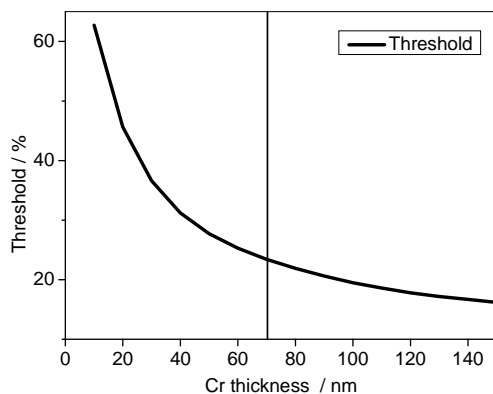


**Fig. 4** The influence of the thickness of the chrome layer on the threshold, calculated for homogeneous chrome.

We also modeled the influence of a finite edge slope on the correct threshold criterion. For this purpose we simulated the optical image for line structures with a trapezoidal cross section with different edge slopes  $\alpha$  (see figure 5, left). The nominal medium linewidth of the line structure taken at a height of 50 % was 1  $\mu\text{m}$ . The edge angle  $\alpha$  was varied from 30° to 90°. The variation of the threshold in dependence of  $\alpha$  is depicted in Figure 5 (right). For high quality edges with edge slopes of  $> 70^\circ$  we derive a remaining linewidth error of  $< 9.6$  nm ( $k=2$ ) due to the finite edge slope. The influence of this parameter could be significantly reduced by a determination of the average slope of the structure edges e.g. using an AFM.

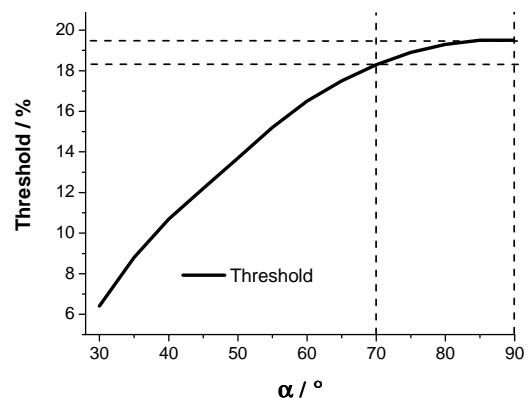
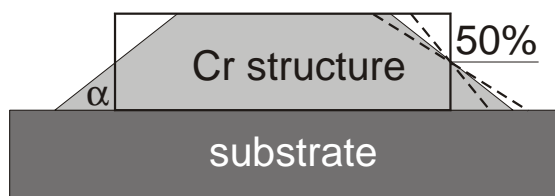


**Fig. 5** Variation of the edge angle  $\alpha$ , the nominal linewidth of 1  $\mu\text{m}$  was fixed at a height of 50 % (above). Variation of the threshold in dependence of  $\alpha$  (right).

### 3.2 Low voltage scanning electron microscopy at PTB

#### Operation principle

In scanning electron microscopy, a focused electron beam with a diameter of a few nanometers is scanned over the specimen surface while the signal of the secondary electrons (SE) emitting from the specimen surface is recorded by a scintillation detector (i.e. beam-scan method in contrast to object-scan method described in the above paragraph). Thus, the instrument registers an intensity profile that indicates the local SE yield as a function of the scan position. The local SE yield is affected both by the local surface topography and by material properties. Therefore, proper physical modelling is necessary to set the yield in correlation with the specimen properties and to derive correct CD values.

The SEM used at PTB for CD calibration of photomasks is designed for low voltage operation, i.e. the beam electrons have an energy of typically 1 keV. Low voltage SEM has the advantages of being a very surface-sensitive method due to the low penetration depth of electrons and the resulting high yield of secondary electrons. Thus it provides a good signal to noise ratio at low probe currents below 10 pA and particularly it reduces specimen charging significantly. The instrument is equipped with an on-axis scintillation detector that shows neither anisotropic yield nor shadowing, so image analysis is independent of azimuthal specimen orientation. The SEM measuring system (called Electron Optical Measuring System, EOMS) is described in detail in [13]. The calibration of scan position as well as the detection (and correction) of scan field distortions is done by means of the instrument's laser interferometer controlled specimen stage.

#### Physical modelling

Due to the complex process of image formation, SEM images have to be interpreted carefully. Therefore, a detailed physical model of image formation was developed which is based on Monte Carlo simulations. In the simulation, the diffusion of beam electrons within the specimen as well as excitation and emission of secondary electrons is modeled. The intensity of the calculated secondary electron signal is recorded as a function of scan position and is used for a direct comparison with measured signal profiles or for the generation of synthetic SEM images (for testing of CD evaluation algorithms). Monte Carlo simulations of signal formation were performed with the program package MOCASIM [14]. The simulation offers a free configuration of specimen geometry and detector strategy. The specimen geometry is stored in a matrix with a cell size of typically 0.5 or 1 nm. The specimen can be composed of up to four materials with a free elemental composition. In the model, specimen topography is defined by structure height, top linewidth (as the distance of left and right top corner position), top corner rounding radius, and edge slope angle (Fig.6). The top edge position is defined as the intersection point of the tangent terminating the upper plateau with the edge slope tangent. Therefore, the corner roundness does not affect the position of the top edge.

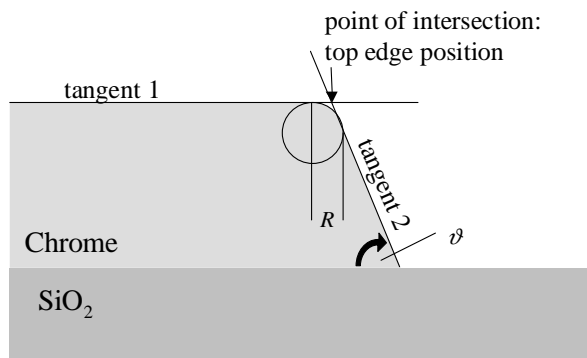


**Fig. 6** Definition of top edge position in the model. Tangent 1 terminates the upper plateau of the structure, tangent 2 is the edge slope tangent,  $\alpha$  the slope angle, and  $R$  the top corner radius. The point of intersection of the two tangents defines the top edge position.

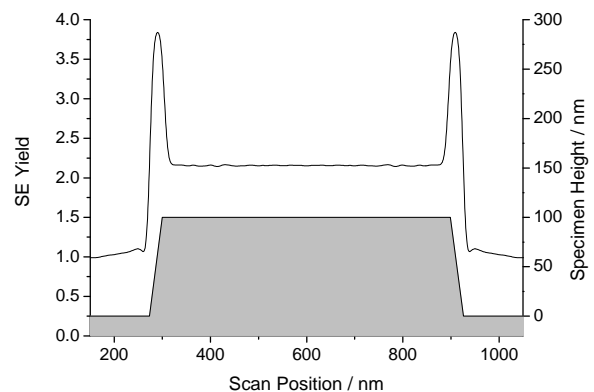


**Fig. 7** Monte Carlo calculated signal profile for an opaque 600 nm chromium line on quartz, edge slope  $80^\circ$ , no top corner rounding, e-beam diameter 10 nm FWHM, electron energy 1 keV (Note: the characteristic local minimum at the bottom usually is not detectable with EOMS system).

#### Formation of edge peaks and top CD definition

The most prominent feature of SEM intensity profiles at CD structures is a distinctive signal peak at the structure edges. Fig. 7 shows the topography of a chromium line on quartz substrate and the associated signal profile in a Monte Carlo simulation. The peak's inner, exponential rising flanks are the result of electron diffusion through

the edge, the peak's decay length is determined the mean electron free path and the peak maximum is reached directly at the end of the upper plateau. It has been shown that the exponential behavior of the edge peak flanks is a result solely of the basic mechanism of electron diffusion in solid state and is therefore largely independent of specimen features as material composition, edge slope, etc. In consequence, a robust and well defined edge criterion can be derived from the diffusion peak.

An exponential function is approximated to the inner, exponential growing flank of the edge peaks (Fig. 8). The fit range is restricted to values below a threshold of 50 %-75 % of the peak maximum. Thus, deviations from the exponential behavior near the peak maximum due to the SEM's finite resolution are excluded from fitting. The approximated function is then extrapolated to a value of 100 % peak maximum and this position is defined as top edge position. The distance of left and right top edge position is defined as top CD. Top CD linewidth measurements based on the exponential fit CD operator already showed good conformity with AFM measurements at silicon structures [15].

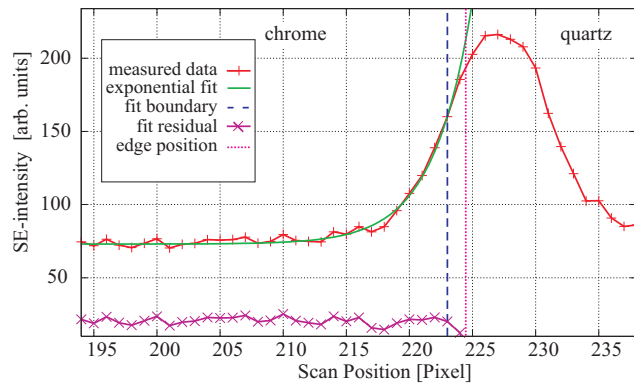


**Fig. 8** Experimental determination of top CD. An exponential function is approximated to the experimental data. The fit range is restricted to values below 65 % of the peak maximum, extrapolation to 100 % peak maximum defines the top edge position.

### Top CD uncertainty evaluation

In addition to the uncertainty analysis for the case of the UV microscope, the SEM measurement uncertainty budget of top CD was derived in a similar way. Details of this analysis were already described before [10]. The largest uncertainty contributions are due to the instrument reproducibility and the influence of line width variation over the 5  $\mu\text{m}$  line sections measured on different masks. Measurement uncertainties of around 15 nm or even better on very good line structures can be achieved for top CD.

For typical edge slopes of  $60^\circ - 80^\circ$ , top CD measurement results are only little affected by the probe diameter. Only very steep edges (slope angle  $> 85^\circ$ ) show a stronger effect. For such edges, the projection of the edge transition is smaller than the probe diameter and a loss of peak maximum intensity results due to resolution limitation. In consequence, the fitting range is shifted and the top CD value shifts about 10 nm for a probe diameter of 10 nm. Thus for the case of steep edges, a correction of the exponential top CD edge operator is required and was already published [16]. The trends in CD variation due to variation of model parameters which are presented here are confirmed by other Monte Carlo investigations for silicon structures and bottom CD evaluation [17].

## 4. RESULTS OF ROUND ROBIN MEASUREMENTS

### 4.1 Description of differences between reference CD photomask standards

Different mask blanks and different mask production processes were used by some of the project partners to produce a set of five CD reference standards for all project partners. However all standards had the identical layout, which was developed jointly before. The PTB calibrated line and space structures on these photomask standards by means of UV transmission microscopy (CD defined as width of structure at 50% height) and SEM (top CD). Additionally edge slope angles were measured by AFM at some line structures on these masks. The partners were provided with calibration reports on the measurement results of their reference standards and were asked to calibrate the unknown CD mask by referring to their reference masks. Table 1 shows the characteristics and use of the CD reference masks and the round robin mask. The uncertainties for layer thickness are about 2 nm and about  $5^\circ$  for edge slope.

In view of the parameter dependencies of optical transmission microscopy shown in figures 4 and 5 it could be expected, that systematic calibration differences would occur if the structures on a reference mask would have other dimensional parameters (height, slope) than on the round robin mask. Table 2 provides an overview of these theoretical corrections of systematic differences.

CD Masks	Ref. mask #1	Ref. mask #2	Ref. mask #3	Ref. mask #4	Ref. mask #5	Round Robin
Blank manuf.	1	2	1	1	1	1
Mask manuf.	1	2	3	1	1	1
AR Cr layer thickness / nm	73	100	70	73	73	73
Edge slope / °	73	74	90	73	74	71
Use of partner	A	B, C	D	E	F	all

**Table 1:** Characteristics and use of the CD reference masks and the round robin mask. Also given are the theoretically expected CD corrections for opaque single lines which have to be taken into account for optical transmission microscopy if reference structures and structures on the round robin mask show different topography.

Partner		A	B	C	D	E	F
CD metrology tool		SEM	UV	DUV	UV	AFM (@ 50 % height)	DUV DUV-WI
CD correction due to: / nm	Top CD	+ 25	-	-	-	-	
	Layer thickness	-	+ 22	+ 22	- 2	-	0
	Edge slope	-	- 2	- 2	- 6	-	-2

**Table 2:** The theoretically expected CD corrections for opaque single lines are given, which have to be applied for optical transmission microscopy if reference structures and structures on the round robin mask show different topography (corrections calculated on the basis of PTB UV microscope setup). Moreover, corrections to transform top CD values to structure width at 50% height are specified for the round robin mask, too.

## 4.2 Presentation of round robin results

In the following figures 9-12, the measurement results on the round robin mask are presented for different types of line/space structures as they were provided, i.e. with the calibration routines applied by the participants using their respective PTB calibrated reference masks (see table 1) but without any further corrections. SEM results refer to top CD while all other results should provide the structure widths at 50% height.

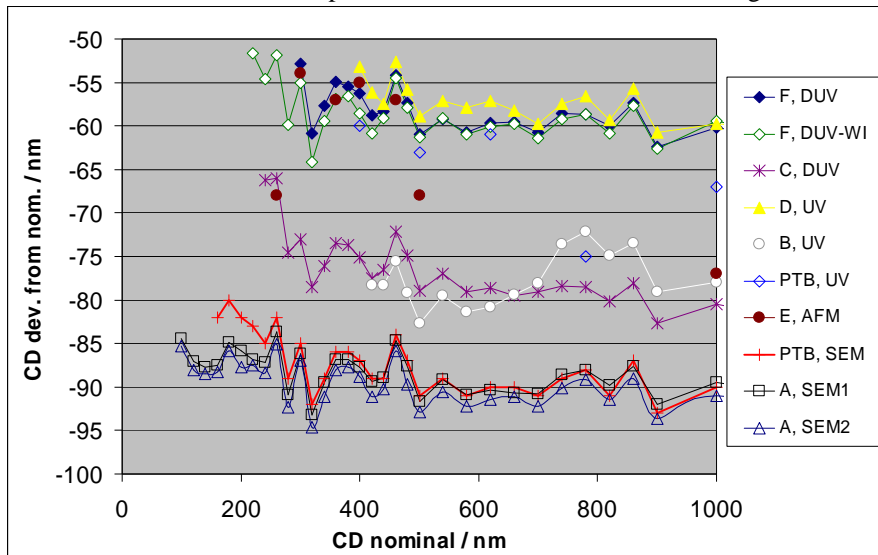


**Fig. 9** Round Robin measurement results on a COG mask standard for **isolated opaque** line structures.

The optical measurement results show a splitting into two groups, separated by about 20 nm. The participants B and C which used a 100 nm thick Cr reference mask measure consistently smaller widths of opaque line structures in comparison to those which calibrated their optical equipment with reference masks of similar Cr layer thickness. The calibration results of participants D and F are in good agreement with the PTB UV microscopy results. Results of the *new water immersion CD metrology tool* were referred to the calibrated DUV tool of participant F, because the immersion tool measurements were pitch calibrated only (50% threshold).

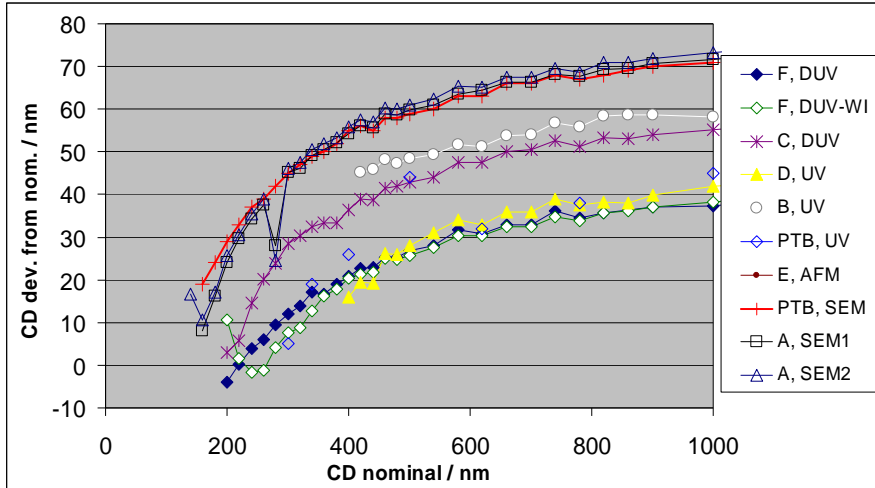


**Fig. 10** Round Robin measurement results on a COG mask standard for **isolated clear** line structures (the differences for the SEM results at nominally 280 nm structure are caused by a particle contamination).

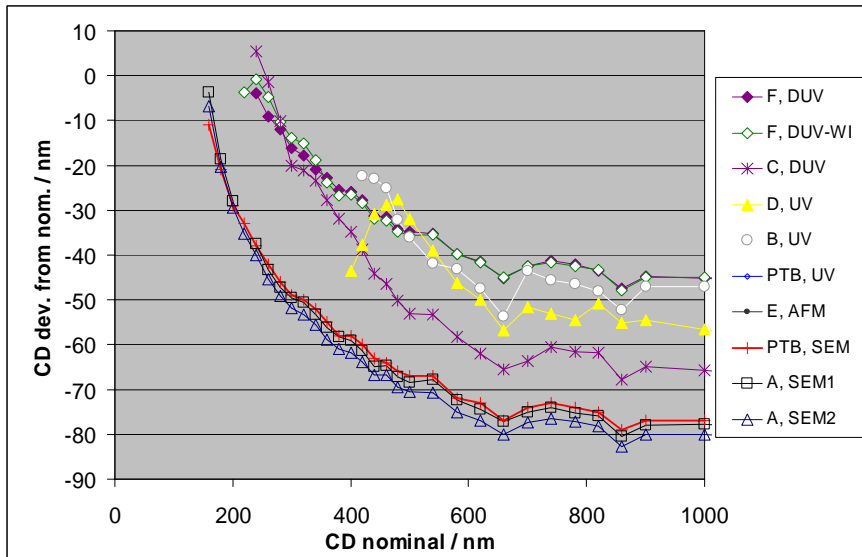


**Fig. 11** Round Robin measurement results on a COG mask standard for **dense opaque** line structures.

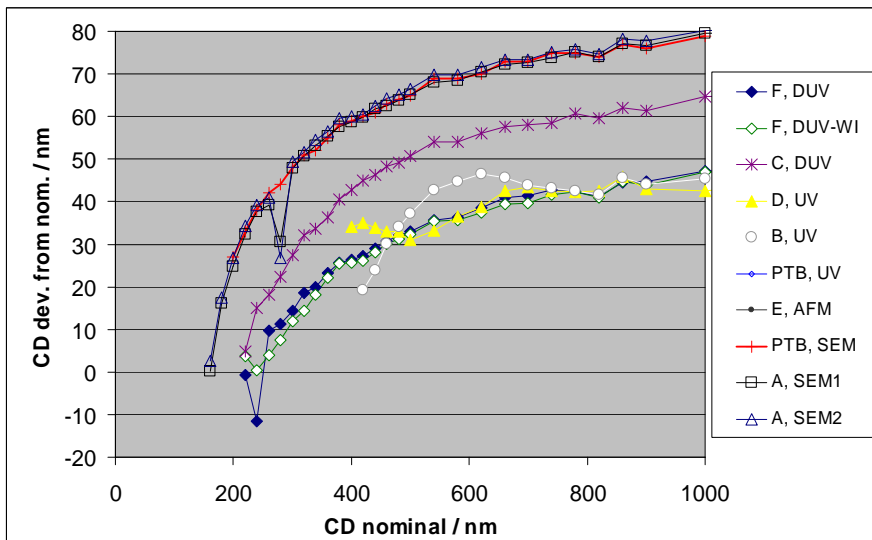


**Fig. 12** Round Robin measurement results on a COG mask standard for **dense clear** line structures.

The observed results could be expected, see table 2. Furthermore, the difference between top CD and CD measured at 50% height was expected to be about 25 nm, deduced from Cr layer height and edge angle. The measured mean differences of the PTB results for top CD measured by SEM and CD at 50% height measured by UV microscopy on isolated structures were determined to be 24 nm for opaque and 29 nm for clear structures. This is a satisfactory agreement taking into account the evaluated respective PTB calibration uncertainties of 15 nm and 25 nm. The agreement between the SEM results of participant A and the PTB also is satisfactory. However for structure widths well below 200 nm deviations occur, which can be explained by the interaction of the electron diffusion cloud over the width of the smallest structures and the influence of this “proximity effect” on the exponential top CD operator of the PTB. Work is going on to properly address this challenge for future calibrations.

### 4.3 Further analysis of round robin results

It is interesting to apply the expected corrections from table 2 to the results of the round robin measurements and to analyse the achieved agreement. Figure 13 shows the results of such an analysis. The mean range of all results after application of the described absolute matching correction now is about 10 nm and the mean standard deviation is below 5 nm. In our opinion this is a quite remarkable and promising result, especially taking into account that the time frame between PTB calibration of some of the reference standards and the round robin exercise was more than one year.

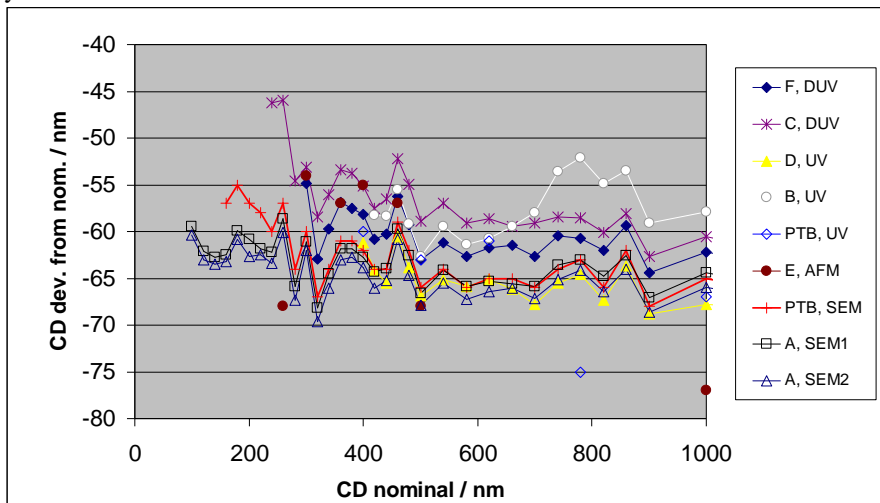


**Fig. 13** Round Robin measurement results on a COG mask standard after application of corrections of expected systematic differences (see table 2) for **isolated opaque** line structures.

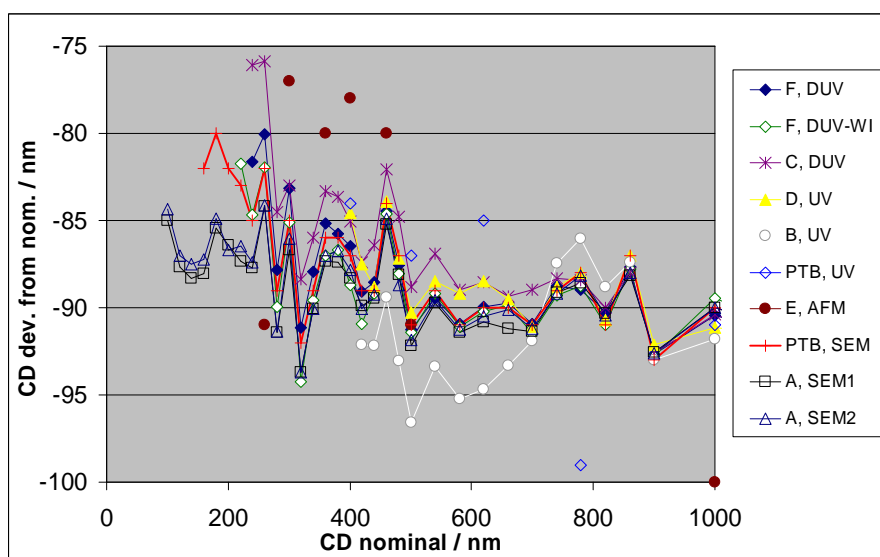


**Fig. 14** Deviations of all round robin results on a COG mask standard for **isolated opaque** line structures, CD offsets are referred to the width of structures between 820 nm and 1 μm as measured by the PTB SEM.

In Fig. 14 we referred all participants results to the mean of PTB SEM results at larger structures between 820 nm and 1  $\mu\text{m}$ , just to define one reference CD and to investigate the deviations of the different tools, including the new DUV immersion equipment, which is compared here for the first time.

The final figure 15 shows measurement results from some partners on a 193 nm attenuated phase shift mask, including results from an AIMS 193 mask metrology tool. Only partner H had used an optically calibrated PTB phase shift mask for CD reference, the other partners used either a fixed 50% threshold criterion (DUV tools, only pitch calibrated) or the isofocal point analysis for determination of an effective CD (AIMS tool). The PTB SEM values again determined the top CD and are in close agreement to the values of participant H, taking into account the expected difference of about 25 nm between top CD and width at 50% height (similar layer thickness and edge angle as for COG round robin mask).

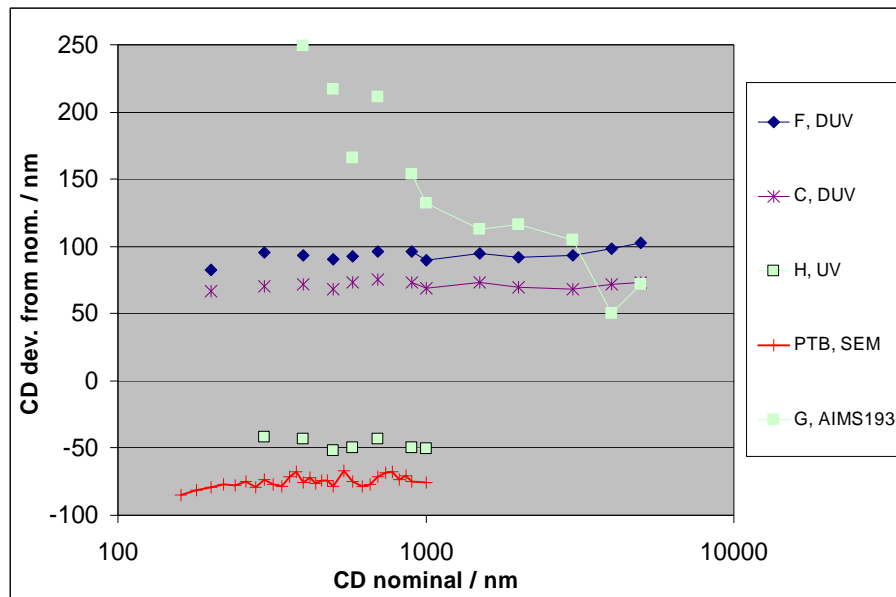


**Fig. 15** CD measurement results on an attenuated PSM mask standard for **isolated opaque** line structures, see text for details. Please note logarithmic CD-scale.

## 5. CONCLUSION AND OUTLOOK

A round robin measurement of a newly developed CD photomask standard was conducted to investigate and demonstrate the performance of the standard and of the instrumentation and calibration procedures involved. Reference CD masks were calibrated by the PTB by different methods, both providing independently traceable calibration results. These reference masks were used by the participants to calibrate their instrumentation before a round robin mask was measured and compared. Correcting for systematic differences one would theoretically expect, the observed range of agreement of all methods applied was better than 10 nm, much better than the estimated measurement uncertainties of the PTB calibrations. Further investigations are on the way to improve the correlation of results of the dedicated CD metrology equipment to the AIMS measurement results.

The round robin exercise clearly indicates the appropriateness of the developed CD mask standard as well as the developed calibration methods for current requirements in CD metrology. The developed standards and calibration methods can also be used by interested third parties.

## 6. ACKNOWLEDGEMENTS

This work was partly funded by the German Ministry of Economics and Labour (BMWA).

## 7. REFERENCES

1. Schätz, Th. et al: "Development and characterization of new CD mask standard: a status report" Proc. 19th EMC, GMM-Fachbericht 39, 37-45, 2003
2. F. Hillmann et al: "DUV Water Immersion Technology Extends Linearity, First Results from the new 65nm Node CD Metrology System LWM500 WI", Proc. EMLC 2005, Dresden, this conference
3. SEMI standard, SEMI P43-0304 - Photomask Qualification Terminology, [www.semi.org](http://www.semi.org)
4. B. Bodermann, E. Buhr, W. Mirandé: "Quantitative Mikroskopie: Dimensionelle Messtechnik an Mikro- und Nanostrukturen", PTB Mitteilungen 113, 4, 9-17 (2003) (in German)
5. M. G. Moharam, E. B. Grann, D. A. Pommet, T. K. Gaylord: "Formulation for stable and efficient implementation of the rigorous coupled-wave analysis of binary gratings", JOSA A 12, (1995), 1068-1076
6. M. G. Moharam, E. B. Grann, D. A. Pommet, T. K. Gaylord: "Stable implementation of the rigorous coupled-wave analysis for surface-relief gratings: enhanced transmittance matrix approach", JOSA A 12, (1995), 1077-1086
7. P. Lalanne, G. M. Morris: "Highly improved convergence of the coupled-wave method for TM-polarization", JOSA A 13, (1996), 779-784
8. M. Totzeck: "Numerical simulation of high-NA quantitative polarization microscopy and corresponding near-fields", Optik 112, (2001), 399-406
9. ISO 1993 Guide to the Expression of Uncertainty in Measurement (Published by the ISO in the name of the BIPM, IEC, IFCC, IUPAC, IUPAP and OIML (Geneva))
10. W. Mirandé et al: "Characterization of new CD photomask standards", Proc. SPIE Microlithography, Vol. 5375, p. 29-40, 2004
11. J. Potzick, National Institute of Science and Technology, NIST: private communication
12. J. Potzick et al, "New NIST Photomask Linewidth Standard", Proc. SPIE, Vol. 4889, 2002
13. W. Häßler-Grohne, H. Bosse, "Electron optical metrology system for pattern placement measurements", Meas. Sci. Technol. 9, 1120-1128 (1998)
14. L. Reimer, M. Kässens, L. Wiese, "Monte Carlo Program with free Configuration of Specimen Geometry and Detector Signals", Microchim. Acta 13, pp.485-492 (1996)
15. W. Mirandé, C.G. Frase, "Comparison of Linewidth Measurements on Si Structures performed by Atomic Force Microscopy (AFM) and low Voltage Scanning Electron Microscopy (SEM)", Proceedings Quantitative Microscopy (QM '99), Kopenhagen, 1999, PTB-Bericht PTB-F-34, 89-96 (1999)
16. W. Häßler-Grohne, C.G. Frase, K. Hahm, H. Bosse: Analysis and comparison of CD-SEM edge operators: a contribution to feature width metrology, Conf. Proc. Nanoscale 2004, Braunschweig
17. A. Karabekov, O. Zoran, Z. Rosenberg, G. Eytan, "Using Monte Carlo Simulation for Accurate Critical Dimension Metrology of Super Small Isolated Poly-Lines", SCANNING 25, 291-296 (2003)